INTERNAL FIELD ON Hf 177

MEASUREMENT OF INTERNAL FIELD ON HAFNIUM 177 IN GADOLINIUM

by

FAKHR-UN-NISA RAFAI, M.Sc.

A Thesis

Submitted to the Faculty of Graduate Studies

in Partial Fulfilment of the Requirements

for the Degree

Master of Science

McMaster University

November 1969

MASTER OF SCIENCE (1969) McMASTER UNIVERSITY
(Physics) Hamilton, Ontario.

TITLE: Measurement of Internal Field on Hafnium 177 in Gadolinium

AUTHOR: Fakhr-Un-Nisa Rafai, M.Sc. (Punjab)

NUMBER OF PAGES: vi, 56

SCOPE AND CONTENTS:

An alloy of 1% lutecium in 99% gadolinium was made. The rotations of the angular correlation pattern caused by the hyperfine fields acting on hafnium nuclei were measured for the 208-113 keV and 71-250 keV cascades. Using measured data the internal field acting on hafnium in gadolinium and the g-factor for the 250 keV spin 11/2, second excited state, were determined.

The results are as follows:

$$H_{int} = - (252 \pm 14) \text{ kOe}$$

$$g_{11/2} = (.346 \pm .087) .$$

ACKNOWLEDGEMENTS

I wish to thank my supervisor, Dr. J. A. Cameron, for his guidance, assistance and helpful suggestions during the course of this work.

Thanks are due also to the other members of the group for their assistance and to the members of the Atomic Beam Group for their friendly help.

The financial support of the Canadian Commonwealth Scholarship and Fellowship Committee was much appreciated.

Special thanks to my mother, whose constant encouragement and large understanding helped me to do this work.

TABLE OF CONTENTS

LIST OF ILLUSTRATIONS

CHAPTER I

INTRODUCTION

Since the early work by J. V. Dunworth and D. R. Hamilton, in the late thirties, on the angular correlation of successive quanta, this technique has opened several new promising fields of research. In the beginning it was limited to the assignment of spin and parity to nuclear levels. But soon it was found out that the angular correlation pattern is sensitive to extra nuclear fields if the lifetime of the intermediate state is longer than 10^{-10} sec. This effect permits the determination of the g-factor and of the quadrupole moment of excited nuclear states.

E. L. Brady and M. Deutsch, in 1950, did the early work on this effect. But the first measurement was done by the Zurich group,in 1951.

In the rare earth ions, where the paramagnetism is caused by the electrons in the 4f shell, the magnetic field can become as large as 10^{7} gauss. Such large magnetic fields at the nuclei of impurities in ferromagnetic alloys, can be used as perturbing fields to lower the minimum lifetime available for study.

The requirement of this technique is that the atoms

whose nuclei are being studied must be capable of forming alloys with the ferromagnetic materials such as iron, cobalt, nickel or gadolinium.

While many elements are soluble in iron, cobalt or nickel and have been so studied, there is a large class of elements which are not soluble in the metals because of bad mismatch of ionic size and electronegativity. The implantation technique has been used to place the nuclei of such elements into iron and nickel foils by means of acceleration in a mass-separator, for ^{133}Xe[Niesen, 1967], for ^{175}Lu [Deutch, 1966] and for ^{177}Lu by Walter H. Brooker [1967]. Some of these elements are soluble in rare earths. Simplest to deal with is gadolinium since it has the highest Curie temperature and is a simple ferromagnet.

Lutecium, the rare earth metal which is studied here, is capable of alloying with gadolinium.

An alloy of 1% lutecium in 99% gadolinium was made by Research Chemicals, a division of Nuclear Corporation of America. The alloy was tested for homogeneity using electron probe. It was found that the sample was quite homogeneous.

The purpose of the study was to measure (i) the internal field on Hf^{177} in gadolinium and (ii) the g-factor of 250 keV, second excited state of ^{177}Hf.

CHAPTER II

THEORY OF ANGULAR CORRELATION

2.1 The theory of angular correlation as applied to the successive emission of any nuclear radiations was first given by D. Hamilton [Hamilton, 1940]. It was shown that the emission probability of a particle or quantum from a nuclear decay depends, in general, on the angle between the nuclear spin axis and the direction of emission. Under ordinary circumstances the nuclei are randomly oriented, so the radiation is isotropic. An anisotropic radiation is given by a nucleus whose spin axis has a preferred direction in space.

If the nuclei decay through successive emissions R_1 and R_2, then the observation of R_1 in a fixed direction $\bar{K}_1$, chooses nuclei with spins in a preferred direction. Hence the emission of subsequent radiation R_2 will depend on the angle between the direction of emission of the two gamma rays.

A single gamma ray transition, as indicated in figure 1, of angular momentum L, connects two nuclear levels i and f, with spins I_i and I_f. For conservation of angular momentum,

$$\vec{I}_i = \vec{I}_f + \vec{L} \ .$$

The emitted gamma ray is characterized by angular

Figure 1

Single gamma ray transition

Figure 2

Successive emission of two gamma rays

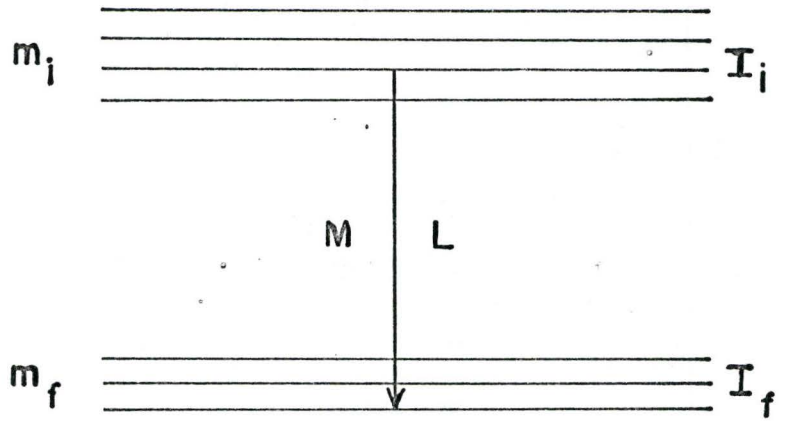
m_i
I_i
M
L
m_f
I_f

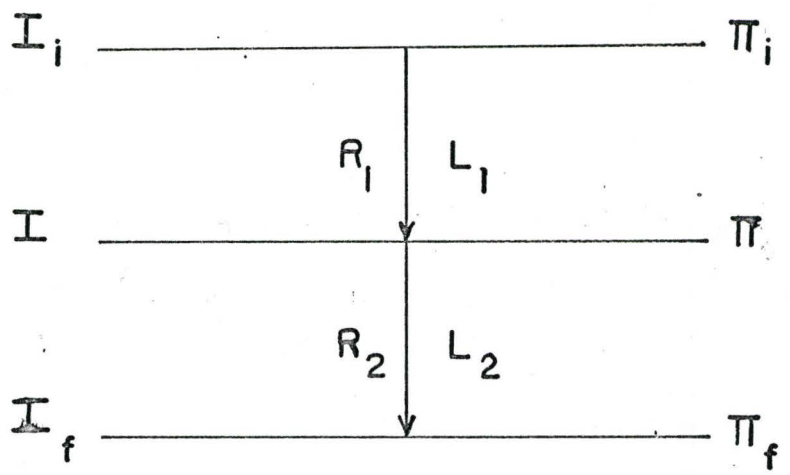
I_i
π_i
R_1
L_1
I
π
R_2
L_2
I_f
π_f

momentum quantum number $\vec{L}$, and magnetic quantum numbers $\vec{M}$, with,

$$\vec{L}^2 = L(L+1)\hbar^2$$

$$\vec{L}_z = M\hbar$$

and $$M = m_i - m_f \ .$$

Each component $[m_i \rightarrow m_f]$ between magnetic sublevels possesses a characteristic directional distribution function $F_L^M(\theta)$, where θ is the angle between the emitted gamma ray and the z-axis. For gamma rays, the distribution function $F_L^M(\theta)$ can be found by calculating the energy flow as a function of θ. The directional distribution of radiation of all multipolarities is given by

$$F_L(\theta) \alpha \sum_{m_i m_f} P(m_i) G(m_i m_f) F_L^M(\theta)$$

where, $P(m_i)$ is the relative population for each sublevel m_i, $G(m_i m_f)$ is the relative transition probability for each component $m_i \rightarrow m_f$ and the gamma ray has multipolarity L.

When a nucleus decays through a cascade $I_i \rightarrow I \rightarrow I_f$, as in figure II, it may do so by successive emission of two gamma rays of multipolarities L_1 and L_2. We may take the direction of the quantization axis to coincide with the direction of emission of the first gamma ray. The directional correlation, $W(\theta)$, between the two gamma rays then becomes identical with the directional distribution function,

$F_L(\theta)$, of the second gamma ray with respect to the z-axis. The directional correlation is,

$$W(\theta) = W(K_1, K_2) = \sum_{K_{even}} A'_{KK} P_K (\cos\theta).$$

The coefficients A'_{KK}'s can be broken up into two factors, each depending on only one transition of the cascade,

$$W(\theta) = 1 + \sum_K A_K^{(1)} A_K^{(2)} P_K(\cos\theta).$$

To introduce normalization of the coefficients, they are so chosen that,

$$A_\infty = 1.$$

There are certain selection rules for the index K,

(i) K is an even integer.

(ii) $0<K<\text{Min}(2I, 2L_1, 2L_2)$.

C. N. Yang, in 1948, has shown that these selection rules follow directly from the invariance of the correlation process under rotation and inversion.

If both the transitions are pure multipoles of order L_1 and L_2 respectively the A coefficients are given by

$$A_K^{(1)} = F_L (L_1, L_1, I_1, I)$$

$$A_K^{(2)} = F_K (L_2, L_2, I_2, I)$$

where the F coefficients are tabulated by M. Ferentz and N. Rosenzweig, 1964. When A coefficients are measured experi-

mentally, then a solid angle correction is applied, and

$$A'_{KK} = Q_{1K} A_K^{(1)} \; Q_{2K} A_K^{(2)}$$

where Q_{1K} and Q_{2K} are solid angle correction factors for transitions 1 and 2.

The most convenient form of describing the directional correlation $W(\theta)$ between two gamma rays is

$$W(\theta) = 1 + A_2 P_2(\cos\theta) + \ldots A_{K_{max}} P_{K_{max}}(\cos\theta).$$

The highest term in this expansion is determined by the selection rule (ii) on page 6 and the requirement that the lifetime of the intermediate level be short for true coincidence to be observed.

The correlation is then expressed as

$$W(\theta) = 1 + A_2 P_2(\cos\theta) + A_4 P_4(\cos\theta).$$

An equivalent expression to this may be written in terms of cosine functions. It will turn out to be a more convenient series in what follows

$$W(\theta) = 1 + B_2 \cos 2\theta + B_4 \cos 4\theta.$$

The B coefficients are related to the A' coefficients by

$$B_2 = \frac{\frac{3}{4} A_2' + \frac{5}{16} A_4'}{1 + \frac{1}{4} A_2' + \frac{9}{64} A_4'}$$

and

$$B_4 = \frac{\frac{35}{64} A_4'}{1 + \frac{1}{4} A_2' + \frac{9}{64} A_4'} .$$

2.2 Perturbed Angular Correlation

If during the lifetime of the excited state concerned, appropriate magnetic or electric fields (external magnetic, internal hyperfine, or both) act on the nuclei, then, the nuclei will precess in these fields, and this will give rise to a change in the angular distribution of the emitted radiation.

If the nucleus is perturbed by a magnetic field H perpendicular to the plane of the two radiations, then its spin axis will precess around this field with the Larmor frequency

$$\omega = \frac{\mu \cdot H}{I\hbar}$$

or

$$\omega = g\mu_N H/\hbar$$

where μ_N is the nuclear magneton, $\hbar$ is Planck's constant divided by 2π, and g is the g-factor of the nucleus. During the time t in the intermediate state, this Larmor precession results in a rotation of angular correlation through the precession angle $\omega_L t$. Hence, instead of the unperturbed

directional correlation $W(\theta,O)$, the rotated correlation pattern

$$W(\theta,H) = W(\theta-\omega t,O)$$

is observed.

In many experiments, including the ones reported here, time τ_o of the coincidence system is much larger than the lifetime of the intermediate nuclear state: $\tau_o >> \tau$. The measured correlation function is then given by the weighted average and is termed the integral angular correlation function.

With a magnetic field directed normal to the correlation plane, the integral angular correlation function has the form

$$W(\theta,H) = \frac{1}{\tau}\int_o^\infty \sum_n B_{2n} \cos 2n(\theta-\omega t)e^{-t/\tau}\, dt$$

$$= \sum_n \frac{B_{2n}}{1 + (2n\omega\tau)^2} (\cos 2n\theta - 2n\omega\tau \sin 2n\theta) .$$

The mean precession angle $\omega\tau$ is measured by

$$R = 2\,\frac{W(\theta,{}^{+}H)-W(\theta,{}^{-}H)}{W(\theta,{}^{+}H)+W(\theta,{}^{-}H)}$$

$$= \frac{\sum_n \frac{B_{2n}}{1 + (2n\omega\tau)^2} 2n\omega\tau \sin 2n\theta}{\sum_n \frac{B_{2n}}{1 + (2n\omega\tau)^2} \cos 2n\theta} .$$

For $\theta = \frac{3\pi}{4}$ this becomes

$$R = 2 \frac{-\frac{B_2}{1 + (2\omega\tau)^2} 2\omega\tau}{B_o - \frac{B_4}{1 + (4\omega\tau)^2}} .$$

For $\theta = \frac{5\pi}{4}$ it becomes

$$R = 2 \frac{\frac{B_2}{1 + (2\omega\tau)^2} 2\omega\tau}{B_o - \frac{B_4}{1 + (4\omega\tau)^2}} .$$

CHAPTER III

RARE EARTH METALS AND FERROMAGNETISM

3.1 Introduction

The angular correlation of a cascade $I_i \rightarrow I \rightarrow I_f$ will, in general, be changed as soon as the nuclei in their intermediate state I are subject to torques, either by external fields or hyperfine fields.

The first investigation on externally applied magnetic fields was made by Goertzel (1946) and further extended by Alder (1952). External fields as large as 53.1 kilogauss were used, by E. Mathias, E. Karlsson and C. A. Lerjefors (1962), to perturb the angular correlation in the 208 keV-113 keV in Hf^{177}.

The angular correlation can also be perturbed by internal magnetic fields acting on nuclei in diamagnetic ions situated as dilute impurities dissolved in ferromagnetic host metals. Most of the work has been done on pure ferromagnetic host metals of the 3d shell, namely iron, cobalt and nickel. This technique is now extended and measurements can be made using internal magnetic fields acting on nuclei of diamagnetic ions dissolved in the ferromagnetic rare earth

metals as gadolinium, terbium, dysprosium, holmium and erbium.

3.2 Rare Earth Metals

The rare earth metals are members of Group III-A elements, whose atomic numbers are 57 through 71. In the fourth and fifth periods no electron is placed in the 4f level, because the 4d, 5s and 5p levels are all energetically lower than the 4f level. In the sixth period the 6s level is filled and one electron enters the 5d level before the 4f level is occupied. At this point the 4f shell is in a lower energy state than the 6s, 5d level, and the filling of the 4f level occurs before another electron is added to the 5d level.

The filling of the 4f level requires 14 electrons. Each rare earth element has essentially the same outermost or valence shell configuration. It is this fact which explains the similarity of the chemical, metallurgical and physical properties of these elements, and any differences must be due, in general, to the number of 4f electrons.

The rare earth metals are generally soft and malleable, but tend to become harder as the atomic number increases. Most of them are paramagnetic, but some of them are ferromagnetic as gadolinium, dysprosium, terbium , and holmium. They are active reducing agents, although they are moderately stable in dry air.

Ionic radii are useful in predicting the alloying behaviour of two metals. If the radii differ by more than 15%, very limited solid solubility is to be expected, but if they differ by less than 15%, then alloying is possible, if other factors are favorable. Atomic radii of Lu and Gd are 1.737 Å and 1.794 Å.

3.3 Ferromagnetism

A ferromagnetic substance is one which has a magnetic moment even in zero applied magnetic field. A spontaneous moment suggests that electron spins and magnetic moments are arranged in a regular manner.

The magnetic susceptibility per unit volume is defined as

$$\chi = M/H$$

where M is the magnetization, which is defined as the magnetic moment per unit volume. H is the magnetic field intensity. In Gaussian units χ is dimensionless. Substances with positive susceptibility are called paramagnetic substances.

The existence of an interaction between elementary dipoles that would lead to their parallel alignment was first postulated by Weiss in 1907. The Weiss field may be considered as equivalent to an effective magnetic field acting on electron spins and Weiss postulated that its strength

should be proportional to the magnetization. Heisenberg,in 1928, studied the problem by quantum-mechanical methods and pointed out that Weiss field is due to quantum mechanical exchange.

Dirac, in 1935, showed that, apart from a constant term, the effective coupling between spins due to the exchange effect is equivalent to a potential energy of the form

$$V_{ij} = - 2J_{ij} (\vec{S}_i \cdot \vec{S}_j)$$

where J_{ij} is the exchange integral connecting atoms i and j, and $\vec{S}_i$ is the spin angular momentum vector of atom i, measured in multiples of the quantum unit $h/2\pi$. There are two noticeable facts about this, one is that the exchange integrals can be fairly large. The other is that the potential is isotropic, or does not depend on how the spins $\vec{S}_i$ and $\vec{S}_j$ are aligned relative to the radius vector $\bar{\gamma}_{ij}$ joining atoms i and j.

From Weiss theory it is known that below the Curie temperature, T_c, the system possesses a spontaneous magnetization, and above the Curie temperature the system is paramagnetic, the magnetic susceptibility becoming infinite as the temperature approaches T_c from above. At temperatures well below the Curie temperature, the magnetic moments of a ferromagnetic substance are completely aligned. However, the overall moment of the substance may be much less than that corresponding to saturation since the moments may not be

parallel. In this case application of an external field causes alignment of the moments, and produces saturation magnetization.

3.4 Hyperfine Fields

The orientation of the nuclei may be regarded as due to an effective magnetic field H which may be written as

$$H_{eff} = H_{\ell} + H_c + H_a \qquad \text{[Marshall,1968]}$$

where H_{ℓ} is the local magnetic field at the position of the nucleus

H_c is the contact field through contact interaction with outer s-electrons,

H_a is the effective field due to the interaction of the nucleus with the electrons on the same atom.

The local magnetic field at the nucleus is given by

$$H_{\ell} = H_e - DM + \frac{4}{3}\pi M + H'$$

where H_e is the external field,

DM the demagnetizing field, depending only on the shape of the specimen,

$\frac{4}{3}\pi M$ is the Lorentz field,

H' is the small residue of the Lorentz field.

For cubic ferromagnets H' is zero, and for hexagonal close packed H' is about 10^{-3} of the Lorentz field. So H' is negligible. The shape of the source was cylindrical, and

it was about 10 times longer than the diameter. So it is considered a long circular cylinder. The value of D for such a shape is zero. The term - DM is then zero. The value of saturation magnetization in gauss is 2 k0e. The term $\frac{4}{3}\pi M$ is then 8 k0e. The external field is 5 k0e. So the local magnetic field at the nucleus, H_ℓ is 13 k0e.

The s conduction electrons, if polarized, make the major contribution to the hyperfine field, acting on the impurity nuclei, through the Fermi contact interaction. Watson and Freeman [1961] have pointed out the possible contribution of a net exchange interaction between the outer polarized core of the rare earth ion and the conduction electrons which might give rise to a negative polarization of the conduction electrons. It seems unlikely, however, that this could be large enough to explain the magnitude of the field observed [S. G. Cohen 1964].

The ferromagnetic interactions in the pure rare earth metals are essentially indirect interactions between the 4f electrons via the conduction electrons. The precise nature of this indirect interaction and the 4f conduction electron interaction, is still to some extent undetermined. For ions with a half closed shell (like Gd and Eu) the dominant contribution arises from the exchange polarization of the core electrons by the unfilled 4f-shell electrons, where as

for the other unfilled 4f-shell elements the dominant contribution comes from the orbital angular momentum of the 4f electrons which, unlike the case for 3d elements, is almost completely unquenched. According to Kasuya and Yosida, in 1964, the local polarization at a particular impurity site can be estimated in terms of the basic effective exchange integral J_{s-f} acting between the 4f electrons and s-conduction electrons.

From the sign and magnitude of the observed hyperfine fields, the sign and the magnitude of J_{s-f} can be deduced, provided other contributions to the hyperfine interactions are small.

CHAPTER IV

THE COLLECTIVE MODEL

4.1 The study of the structure of nuclei includes all aspects of the motion of nucleons, their paths in space, their momenta, the correlation between them, their mutual binding energies. The development of nuclear models has taken place along two lines. The statistical models, in which the constituents of the nucleus are treated on a statistical basis, as in the case of a liquid drop or a volume of gas. Statistical models have been developed for heavy nuclei and have proved to be very successful. The second type of model is the shell model, in which the nucleons are treated as individual particles.

The shell model has been an important guide in the interpretation of nuclear phenomena. The nuclear field is generated by the nucleons themselves. The dynamic aspects of the field, associated with collective oscillations of the structure as a whole, must be expected to play an essential role. The large quadrupole moments of some nuclei and the occurrence of nuclear gamma transitions of electric quadrupole type with very short lifetimes are the evidences of collective aspects of nuclear structure.

The electromagnetic properties of a nucleus can be completely described by specifying its current and charge densities and intrinsic nucleon multipole moments. For the study of nuclear structure the knowledge of electromagnetic multipole moments is not only helpful but is of great importance.

The magnetic dipole moment consists of contributions from the orbital motion of the protons in the nucleus, and from the spins of both protons and neutrons. The magnetic dipole operator is written as

$$\vec{\mu}_{op} = (\vec{\mu}_{orbital})_{op} + (\vec{\mu}_{spin})_{op} \qquad (1)$$

where

$$(\vec{\mu}_{orbital})_{op} = \frac{e}{2MC} \sum_{K=1}^{A} g_L^{(K)} \vec{L}^{(K)} \qquad (2)$$

$$(\vec{\mu}_{spin})_{op} = \frac{e}{2MC} \sum_{K=1}^{A} g_S^{(K)} \vec{S}^{(K)} \quad . \qquad (3)$$

Here $\vec{L}^{(K)}$ and $\vec{S}^{(K)}$ are the orbital angular momentum and spin operators for the K^{th} nucleon, and g_L, g_S are the orbital and spin gyromagnetic ratios.

The magnetic moment μ is defined as the expectation value of the z-component of μ_{op} in nuclear magnetons in the state in which

$$(\mu_{z_{op}}) = \mu_{op}$$

that is

$$\mu = \langle J, m = J | \mu_{z_{op}} | J, m = J \rangle .$$

For a nucleus of zero spin and therefore no preferred orientations, $\mu = 0$.

The electric quadrupole operator is defined by

$$Q_{op} = e \sum_{K=1}^{A} g_L^{(K)} \ (3z_K^2 - r_K^2)$$

where g_L^K is simply added formally so the sum will be over the protons (g_L^K for neutrons = 0

for protons = 1)

The electric quadrupole moment is then given by the expectation value of Q_{op} for the particular nuclear state.

4.2 The Collective Model

The nuclear collective properties can be described by a set of coordinates, α, characterizing the spatial distribution of the nucleon density which, in turn, defines the nuclear field. Such collective coordinates are symmetric functions of the individual nucleon coordinates.

The nuclear surface is defined by

$$R(\theta,\phi) = R_o [1 + \sum_{\lambda=0}^{\infty} \sum_{\mu=-\lambda}^{\lambda} \alpha_{\lambda\mu} \ Y_\lambda^\mu \ (\theta,\phi)]$$

where θ and ϕ are polar angles, R_o is the equilibrium radius, Y_λ^μ the normalized spherical harmonic of order λ, μ and $\alpha_{\lambda\mu}$ are expansion parameters of the nuclear surface. Any collec-

tive motions are expressed by letting $\alpha_{\lambda\mu}$ vary in time.

The important oscillations for the case of non spherical nuclei are those of order 2 associated with quadrupole shapes. In this case, the equation of nuclear surface, referred to the principal axes, is

$$R = R_o[1 + \beta\, Y_2^0\ (\theta)]$$

where β is a measure of the deformation.

The nuclear shape may oscillate about its equilibrium shape or it may rotate without changing the shape or intrinsic configurations, or it may have both motions, oscillation and rotation.

The rotation of the nucleus gives rise to rotational bands or rotational levels associated with each intrinsic state. The energy of such levels is given by

$$E_{rot} = \frac{\hbar^2}{2I}\{J(J+1) - J_o(J_o+1)\}$$

where J and J_o are the spins of a given level and the ground state respectively. The moment of inertia I is much less than the rigid body moment of inertia since a nucleus is not a rigid body. The moments of inertia corresponding to rotational bands vary from one intrinsic state to the other. Such rotational levels are observed in a region away from closed shell, $A \sim 25$, $150<A<190$ and $A>222$.

In these regions, where the distortion parameter, β, is large, the nuclear surface will generally be axially symmetric, and the individual particles with the total angular momentum j, will couple separately to the symmetry axis in states characterized by their component of angular momentum Ω_i along the symmetry axis.

Because of the axial symmetry of the surface, the particle states $+\Omega_i$ and $-\Omega_i$ are degenerate and particles fill these states in pairs.

The nuclear surface may rotate as a whole, and this rotation is characterized by quantum numbers J, K and M, where J is the total angular momentum of the surface plus particles, K is its projection on the body axis, M its projection of a fixed axis in space. In the ground state, then, $K = \Omega$, and R, the surface angular momentum, is zero as shown in the Figure 3.

4.3 Magnetic Moments

In the collective model, the core shares in the angular momentum of the nucleus, and will therefore contribute to the magnetic moment. The contribution to the angular momentum is due both to the neutrons and protons, while the contribution to the magnetic moment is due to the protons alone.

Figure 3

Coupling scheme for deformed nuclei

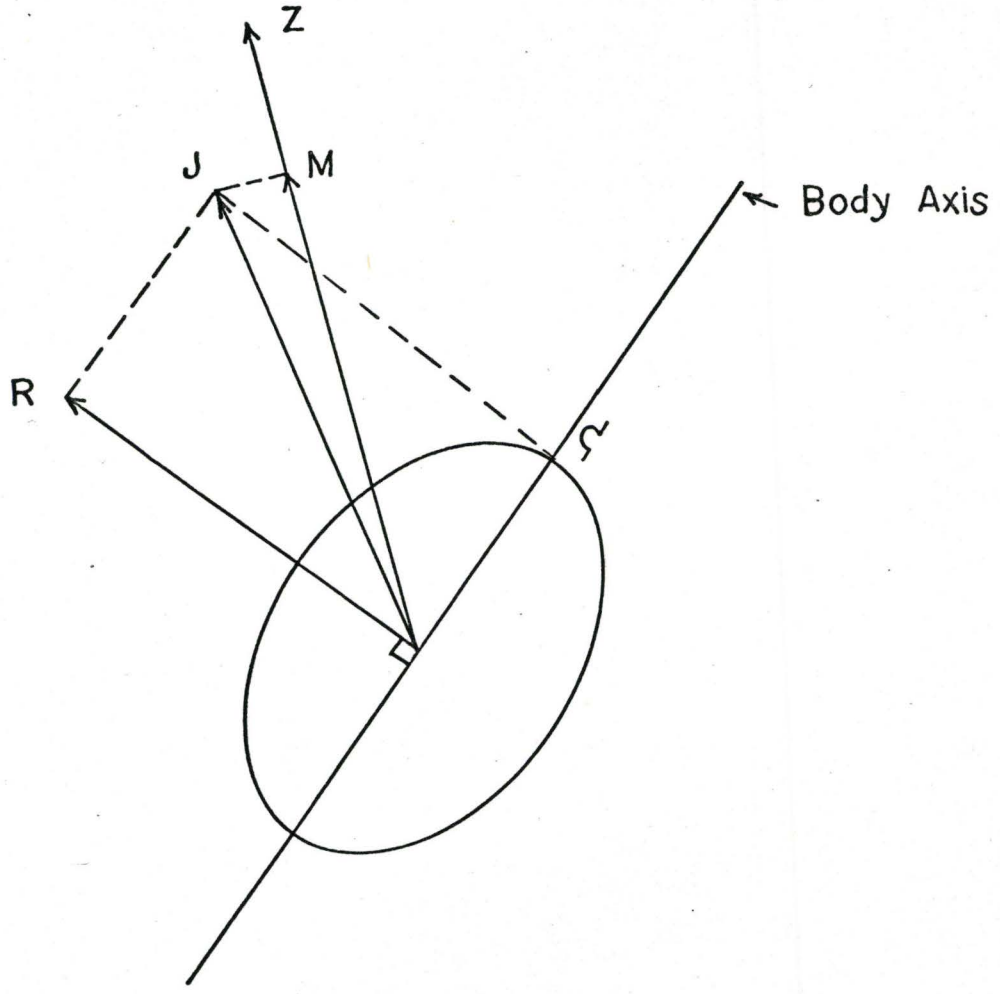
Z
J
M
Body Axis
R
Ω

For a single particle coupled to the surface, the magnetic moment is given by

$$\mu = \langle g_S S_z + g_\ell \ell_z + g_R R_z \rangle_{M=J}. \qquad (4)$$

This we get by generalizing equations 1 to 3, where ℓ_z and S_z denote the intrinsic angular momenta, R_z is the z-component of angular momentum of the core and g_R is the corresponding g-factor.

If the nucleus behaves as a fluid of uniform charge density Z/A, then

$$g = Z/A \ .$$

R may be eliminated from equation (4) by writing

$$\begin{aligned}
\vec{\mu} &= g_s\vec{S} + g_\ell\vec{\ell} + g_R(\vec{J}-\vec{j}) \\
&= g_R\vec{J} + (g_\ell - g_R)\vec{j} + (g_s - g_\ell)\vec{S} \\
&= g_R\vec{J} + (g_s - g_R)\vec{j} + (g_\ell - g_s)\vec{\ell} \\
&= g_R\vec{J} + \vec{G} \ .
\end{aligned}$$

Now, using a wave function $|JMK\rangle$ with one extra-core particle and $K = \Omega$,

$$\begin{aligned}
\mu &= \langle JJK | g_R J_z + G_z | JJK \rangle \\
&= g_R J + \langle JJK | G_z | JJK \rangle .
\end{aligned}$$

G may be written as the spherical tensor G_μ

$$G_o = G_z$$

$$G_{\pm 1} = \mp 2^{-(\frac{1}{2})} (G_x \pm i G_y) .$$

In the body coordinate system, G_μ becomes

$$G_\mu = \sum_\nu D'_{\mu\nu} \; G'_\nu .$$

Defining a gyromagnetic ratio g_K by

$$\langle K | G'_o | K \rangle = K(g_K - g_R)$$

then, the magnetic moment of the nucleus may be written

$$\mu(J,K) = g_R \frac{J(J+1)-K^2}{J+1} + g_K \frac{K^2}{J+1} , \quad K \neq \frac{1}{2} ,$$

and

$$g(J,K) = g_R + \frac{K^2}{J(J+1)} (g_K - g_R) .$$

4.4 Multipole Transitions

The variation of current and charge distributions in the nucleus leads to the emission of radiation which may be classified in electric and magnetic multipoles. The magnetic dipole operator may be calculated from expression (4) and written in terms of the spherical tensor G_μ. The transition rate may be written

$$T(M1) = \frac{16\pi}{9} \frac{k^3}{\hbar} B(M1, J_i K_i \rightarrow J_f K_f)$$

where B(M1) is reduced transition rate - it depends on the square of the reduced matrix element. Within a rotational

band, using the previously defined quantity g_K and the collective gyromagnetic ratio g_R, the expression $\langle K|G_o|K\rangle = K(g_K - g_R)$ holds. Within the band only adjacent levels J and J-1 are connected by M1-transition, and we obtain, for $K \neq \frac{1}{2}$,

$$T(M1) = \frac{16\pi}{9}\frac{k^3}{\hbar}\mu_o^2(g_K - g_R)^2K^2\frac{(J-K)(J+k)}{J(2J+1)}$$

where μ_o is the nuclear magneton.

In heavy nuclei with large collective quadrupole moments, electric quadrupole transitions are usually very strong. The quadrupole moment operator may be expressed as a collective term and a term for extra-core particles as

$$Q_{2\mu} = \sum_p e_p\gamma_p^2 Y_2^\mu(\Omega_p) + ZeR_o^2\alpha^*_{2\mu}$$

where the $\alpha_{2\mu}$ are the collective variables determining the deformed surface and R_o is the average nuclear radius. This precise coefficient comes from the irrotational fluid model, and may therefore be somewhat in error. It is better to derive quadrupole moment operator from observed quadrupole moments.

The quadrupole moment is a tensor of rank two, and therefore $Q_{2\mu}$ in the laboratory system may be expressed in terms of the components $Q'_{2\mu}$ in the intrinsic coordinate system by the transformation.

$$Q_{2\mu} = \sum_{\nu} D^{2}_{\mu\nu} \, Q'_{2\mu}$$

and doing the same analysis as was done previously for B(M1), the B(E2) reduced matrix element may be written

$$B(E2, J_i K \to J_f K) = e^2 Q_o^2 (J_i 2K0 | J_f K)^2$$

for transition in the same band, where Q_o is the intrinsic quadrupole moment characterizing the nuclear deformation and, for the ground state, is selected to the observed quadrupole moment Q by

$$Q = \frac{Q_o J \ (2J-1)}{(J+1)(2J+3)} \ .$$

The transition probability is

$$T(E2) = \frac{4\pi}{75} \frac{1}{\hbar} K^5 \ B(E2).$$

The E2 transition rate is increased over the single-particle value by the full enhancement of collective over single-particle quadrupole moments. Hence, M1 and E2 transitions may compete, and within a band, the mixing ratio δ is given by

$$\delta^2(J \to J-1) = \frac{T(E2, J \to J-1)}{T(M1, J \to J-1)}$$

$$= \frac{3}{20} \left(\frac{\hbar\omega}{mc^2}\right)^2 \left(\frac{Q_o m^2 c^2}{h^2}\right)^2 \frac{1}{(g_K - g_R)^2} \frac{1}{J^2 - 1}$$

The transition rates may be written in terms of τ, the mean life of the decaying states, the total conversion coefficient α_T and the mixing ratio δ^2. The expressions are

$$T(E2) = \frac{1}{\tau} \frac{1}{1+\alpha_T} \frac{\delta^2}{1+\delta^2}$$

and

$$T(M1) = \frac{1}{\tau} \frac{1}{1+\alpha_T} \frac{1}{1+\delta^2} .$$

CHAPTER V

APPARATUS

The experimental arrangement involved the detection of gamma rays, and measurement of their energy and time relationship. For the purpose of this experiment, the two gamma rays in the cascade,discussed in Chapter II, were studied.

5.1 Detector Arrangement

The detectors are 2 inches by 2 inches NaI crystals integrally mounted to an RCA6342A photomuliplier tubes. Each is mounted inside an iron cylinder which can be moved relative to the arm of an aluminium angular correlation table. Thus the distance between the source and the detectors and the angles between the detectors can be changed. One detector is fixed and the other two movable. The distance between the faces of the crystals and the axis about which the two detectors are rotated is kept 7 cms. in the experiment performed here.

The angular correlation table is graduated in degrees. In the centre of the angular correlation table is a cup which holds a post over which the source is mounted at a height corresponding to the mid point of the sodium iodide crystals. The source can be centred by two micrometer screw gauge arrange-

ment. When the source is to be magnetically saturated, the micrometer arrangement is replaced by a liquid nitrogen dewar which holds the electromagnet in it. The source is then placed between the pole tips of the magnet.

5.2 Magnet

The magnet used in the experiment is shown in Figure 4. Each coil has 1000 turns of No. 20 enamelled copper wire wound on a copper former which is thermally connected to the mild steel yoke by copper spacers. The steel yoke has a 1 inch diameter hole cut out at one side and a 1 inch high slit of angular length 130° in the other to allow no hindrance in the gamma rays path to the detectors. The distance between the pole tips can be varied. The electromagnet produces a field of about 2 kOe per amp. The field was kept about 5 kOe, which was sufficient to magnetically saturate the source.

The stray magnetic field at the photomultiplier tube was reduced by a 25 turn compensating coil wound round the outside of the yoke carrying a variable fraction of the magnet current and by the magnetic shielding around the tubes.

5.3 Electronics

The block diagrams of the apparatus is shown in Figure 5. The output pulses from the photo-multipliers are amplified by preamplifiers and a selectable active filter amplifier, in which a bipolar pulse is produced.

Figure 4

The magnet

a) Pole tip

b) The source

c) Bucking coil

d) Magnet coils.

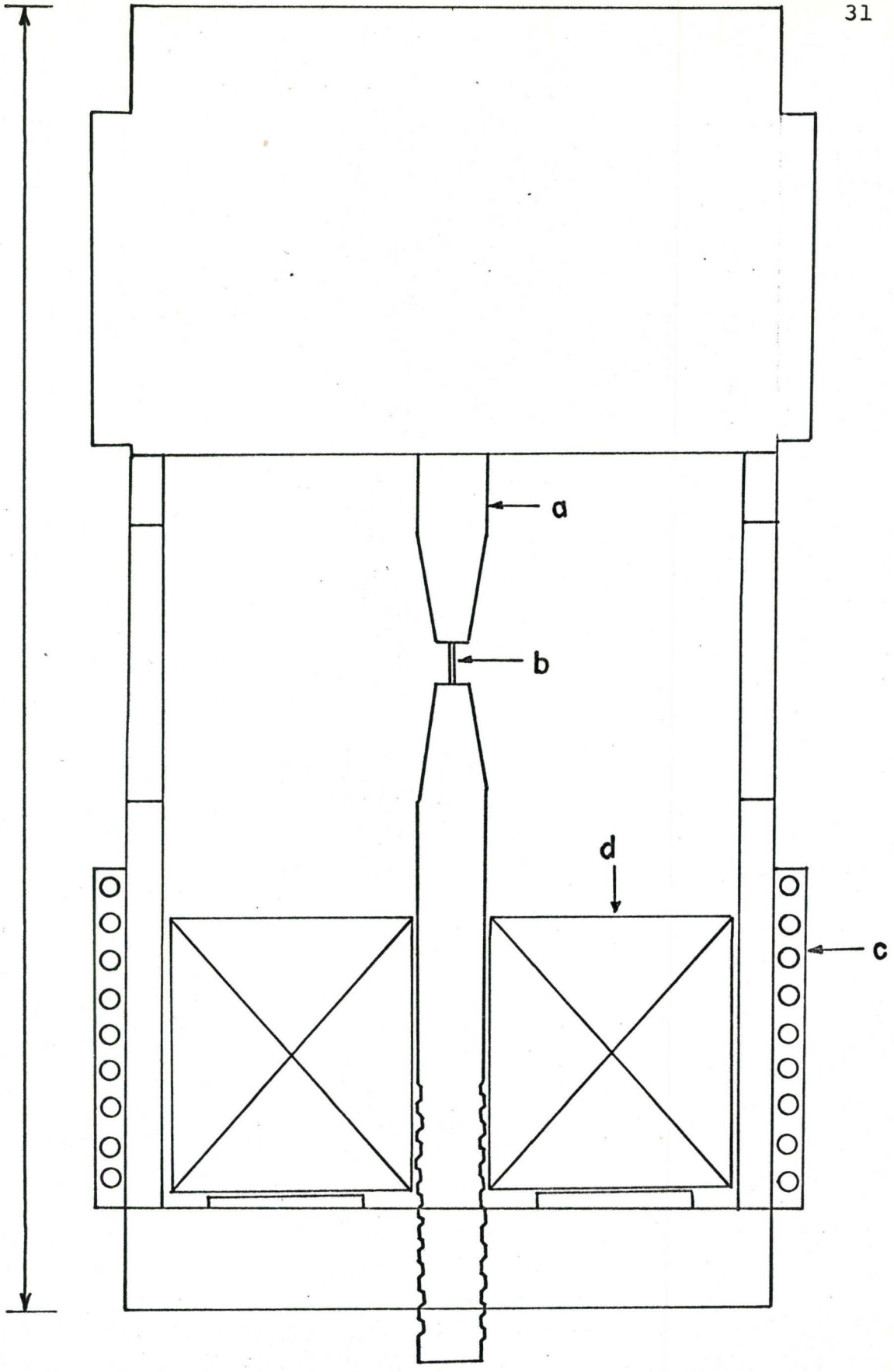
a
b
d
c

Figure 5

The data collecting system

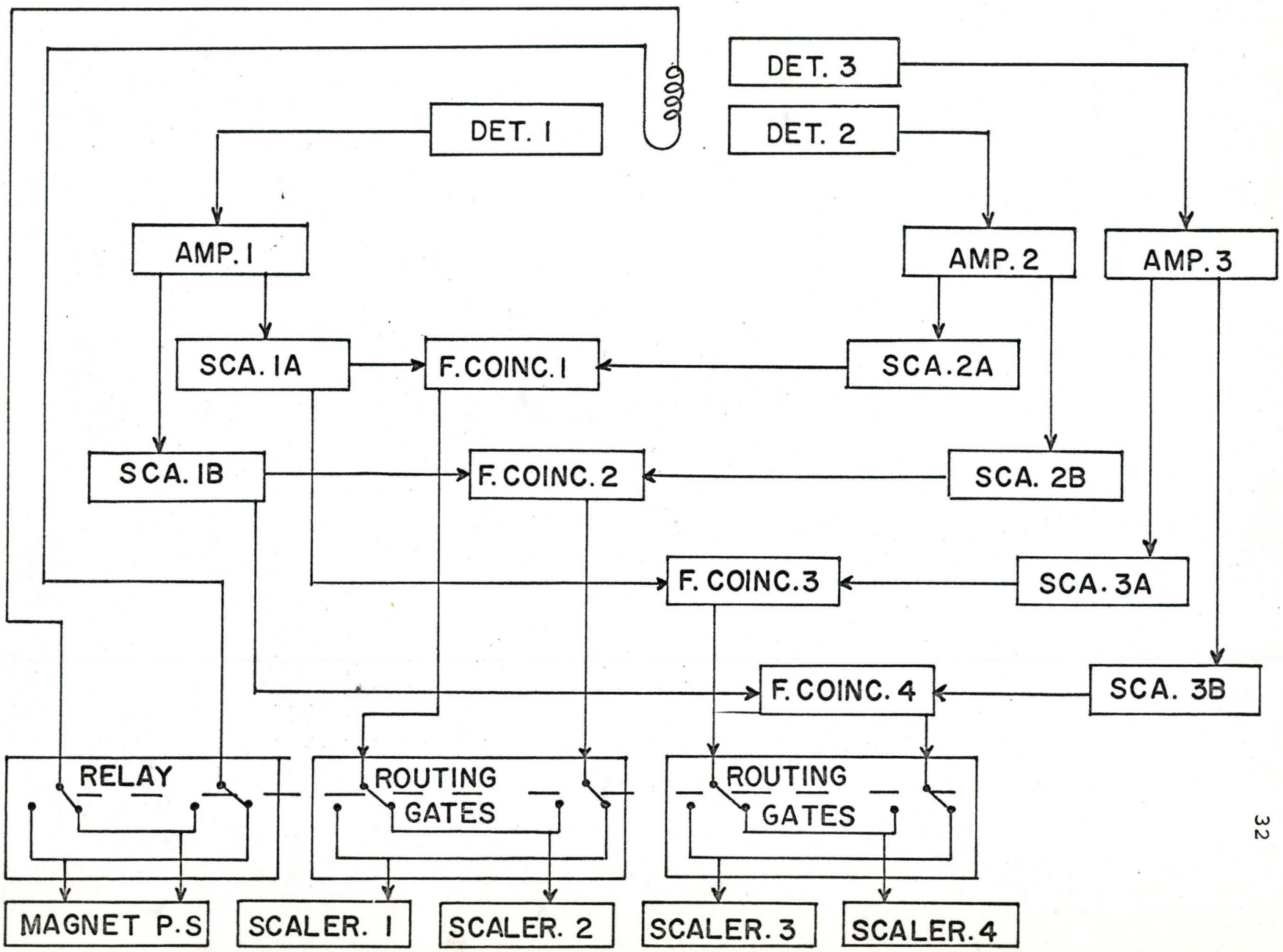
DET. 3
DET. 1
DET. 2
AMP. 1
AMP. 2
AMP. 3
SCA. 1A
F. COINC. 1
SCA. 2A
SCA. 1B
F. COINC. 2
SCA. 2B
F. COINC. 3
SCA. 3A
F. COINC. 4
SCA. 3B
RELAY
ROUTING GATES
ROUTING GATES
MAGNET P.S
SCALER. 1
SCALER. 2
SCALER. 3
SCALER. 4

This pulse is fed to two single channel analyzers, each of which is set to select one of the gamma rays in the cascade being studied. The system is adjusted so that single channel analyzer 1A selects one gamma ray and single channel analyzers 2A and 3A select the second gamma ray in the cascade. Similarly 1B selects one gamma ray and 2B and 3B select the other gamma ray.

The output from one pair of single channel analyzers selecting both gamma rays (e.g. 1A and 2A) is fed into a coincidence circuit. This circuit produces an output pulse whenever a pulse from both single channel analyzers arrives within the resolving time of the circuit ($\sim$ 40 nano secs).

This fast output pulse is then fed to the scalar driver, which produces an output pulse of proper amplitude, width, rise and fall times, which are acceptable to the scalers used for counting the pulses.

The two coincidence outputs, one proportional to $W(\theta,H)$ the other to $W(2\pi-\theta,H)$, the latter being equal to $W(\theta,-H)$. The system is designed in such a way as to switch the inputs to the scalers 1 and 2, and scalers 3 and 4 every time the field direction is reversed. When the field direction is down, the coincidence inputs 1, 2, 3 and 4 are directed to scalers 1, 2, 3 and 4 respectively. When the field direction is up, the coincidence inputs 1, 2, 3 and 4

are directed to scalers 2, 1, 4 and 3 respectively.

A 512 channel analyzer was used to select base lines and window widths for all of the single channel analyzers and also to obtain singles and coincidence spectra.

During magnetic precession measurements the position of the counters are fixed at positions which maximize R. During angular correlation measurements, the counter angles are changed automatically.

CHAPTER VI

EXPERIMENTS AND RESULTS

6.1 Introduction

The decay scheme for the ^{177}Lu ground state, showing the cascades studied in this experiment, their spin sequence, parities and multipolarities, is given in figure 7. The g-factor of 113 keV state of ^{177}Hf is known from external field measurements so $\omega\tau_{113}$ gives the internal field, H_{int}, on ^{177}Hf in gadolinium. The g-factor of 250 keV state is to be measured.

The angular correlation of the 208-113 keV cascades of ^{177}Hf has previously been measured by Matthias, Karlsson and Lerjefors [1962] and found to be:

$$1 - (0.101 \pm .001)\cos 2\theta.$$

For the 71-250 keV cascade, the angular correlation function obtained in previous measurements were

$$1 - (.09 \pm .01)\cos 2\theta$$

by S. Ofer in 1957 and

$$1 - (.085 \pm .009)\cos 2\theta$$

by Brooker in 1967.

Figure 6

The decay scheme of ^{177}Lu

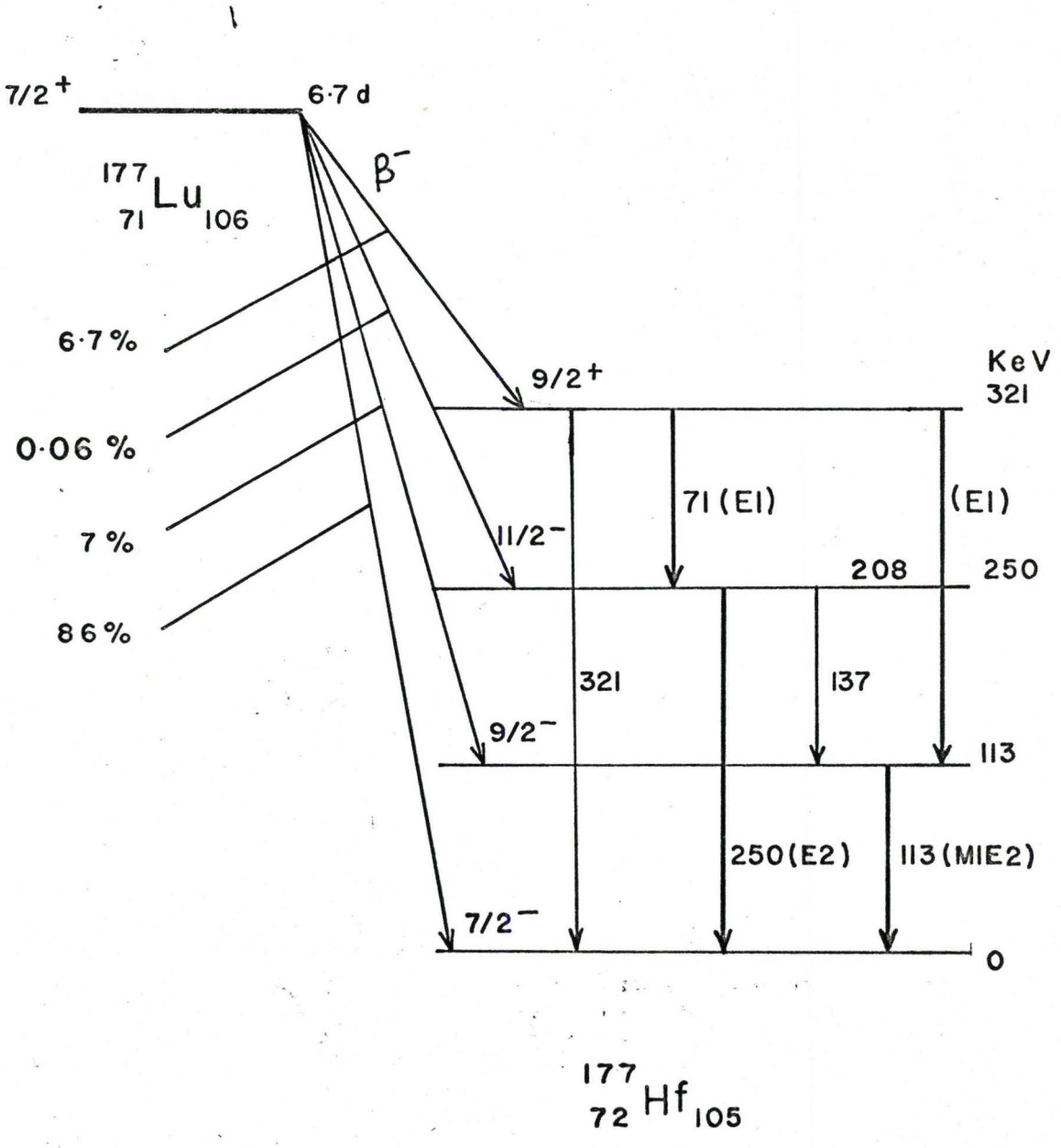
7/2+
6·7 d
β⁻
177 71 Lu 106
6·7 %
0·06 %
7 %
86 %
9/2+
KeV
321
11/2−
71 (E1)
(E1)
208
250
321
137
9/2−
113
250(E2)
113(MIE2)
7/2−
0
177 72 Hf 105

6.2 Angular Correlation Measurements

The angular correlation has been measured for both the 208-113 keV and the 71-250 keV cascades, using a lutecium metal source. The source was prepared by neutron activation of a 10 milligrams lutecium metal sample, in powder form, in the McMaster reactor, and had activity of about 100 micro-curies. The coincidence rate as a function of θ, the angle between the detectors, was found using single channel analyzer windows as shown in figures 8 and 9. A least squares curve was fitted to these data and the results are given in the later sections.

The angular correlation for the 208-113 keV was found to be

$$W\theta = 1 - (0.101 \pm .002)\cos 2\theta$$

which agrees with the results of Matthias, Karlsson and Lerjefors [1952]. The same measurement performed using a lutecium and gadolinium alloy source, gave an attenuated pattern, and B_2 was found to be about 5 percent smaller than the above values. This may be due to the difference in the radiation damage to the two sources.

The angular correlation pattern for the 71-250 keV cascade was found to have the form

$$W(\theta) = 1 - (0.0327 \pm .005)\cos 2\theta.$$

The value of B_2 was found to be about 60 percent smaller than the value obtained by Brooker [1967]. In order to

Figure 7

The coincidence spectra showing spectra in coincidence with windows A and B

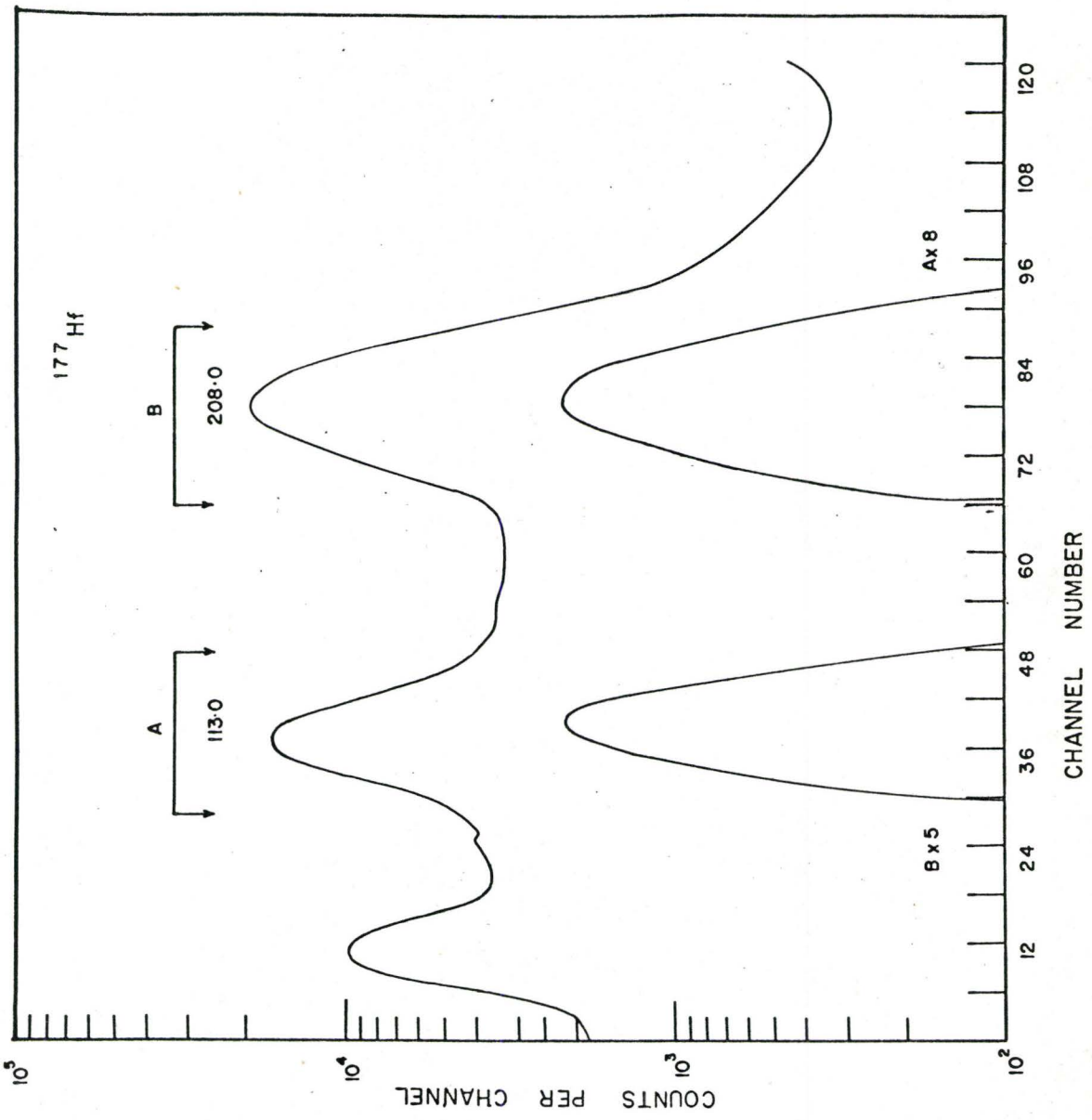
177 Hf
A
113·0
B
208·0
B x 5
A x 8
COUNTS PER CHANNEL
CHANNEL NUMBER
10^5
10^4
10^3
10^2
12
24
36
48
60
72
84
96
108
120

Figure 8

Coincidence spectra showing spectra in coincidence with windows C and D

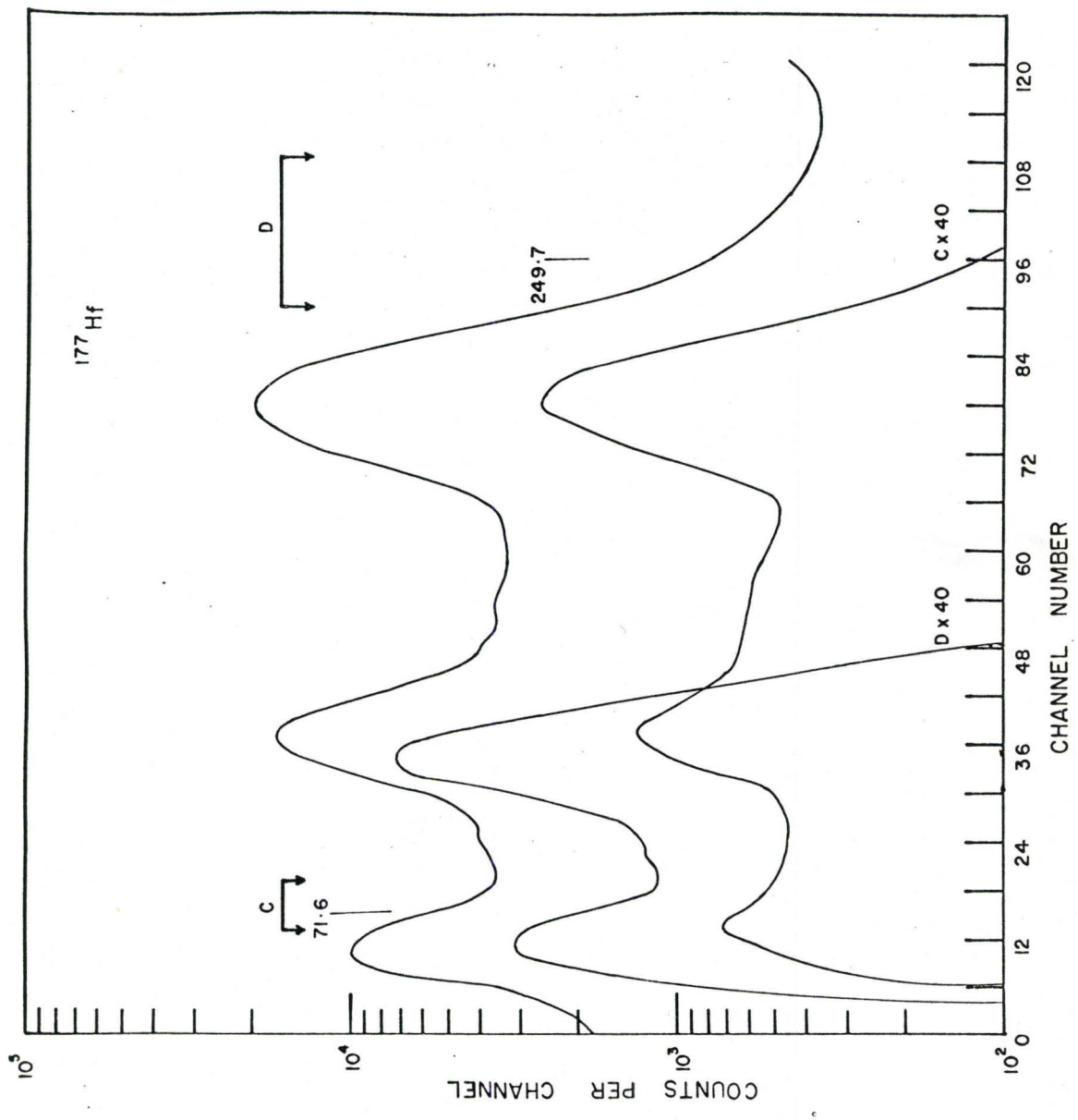
^{177}Hf
C
71·6
D
249·7
C x 40
D x 40
COUNTS PER CHANNEL
CHANNEL NUMBER
10^5
10^4
10^3
10^2
0
12
24
36
48
60
72
84
96
108
120

investigate the source of the discrepancy, the same measurement was performed for several window widths and positions. It was found that as the window widths were decreased and their positions were moved away from the high peaks, the value of B_2 decreases. It seems that Brooker was getting the effects of high peaks which made his value of B_2 larger.

These values have not been corrected for the finite solid angles subtended by the detectors or for the presence of other cascades. The errors include statistical uncertainties and allowances for small changes in window positions and width. The angular correlation patterns are given in figures 10 and 11.

6.3 Perturbed Angular Correlation Measurements

The source for magnetic perturbation experiments was prepared from an alloy of 1% lutecium in 99% gadolinium, which was made by Research Chemicals, a division of Nuclear Corporation of America. A 10 milligrams piece of the sample was machined to a thin cylinder, about 4 millimeters long and about 0.5 millimeters in diameter. This source was placed between the pole tips of the magnet so that the magnetic field was parallel to the geometric axis of the cylinder. In this configuration, the demagnetization factor D is very nearly zero.

In order to ensure that the gadolinium alloy could be

Figure 9

The angular correlation pattern for the

208-113 keV cascade

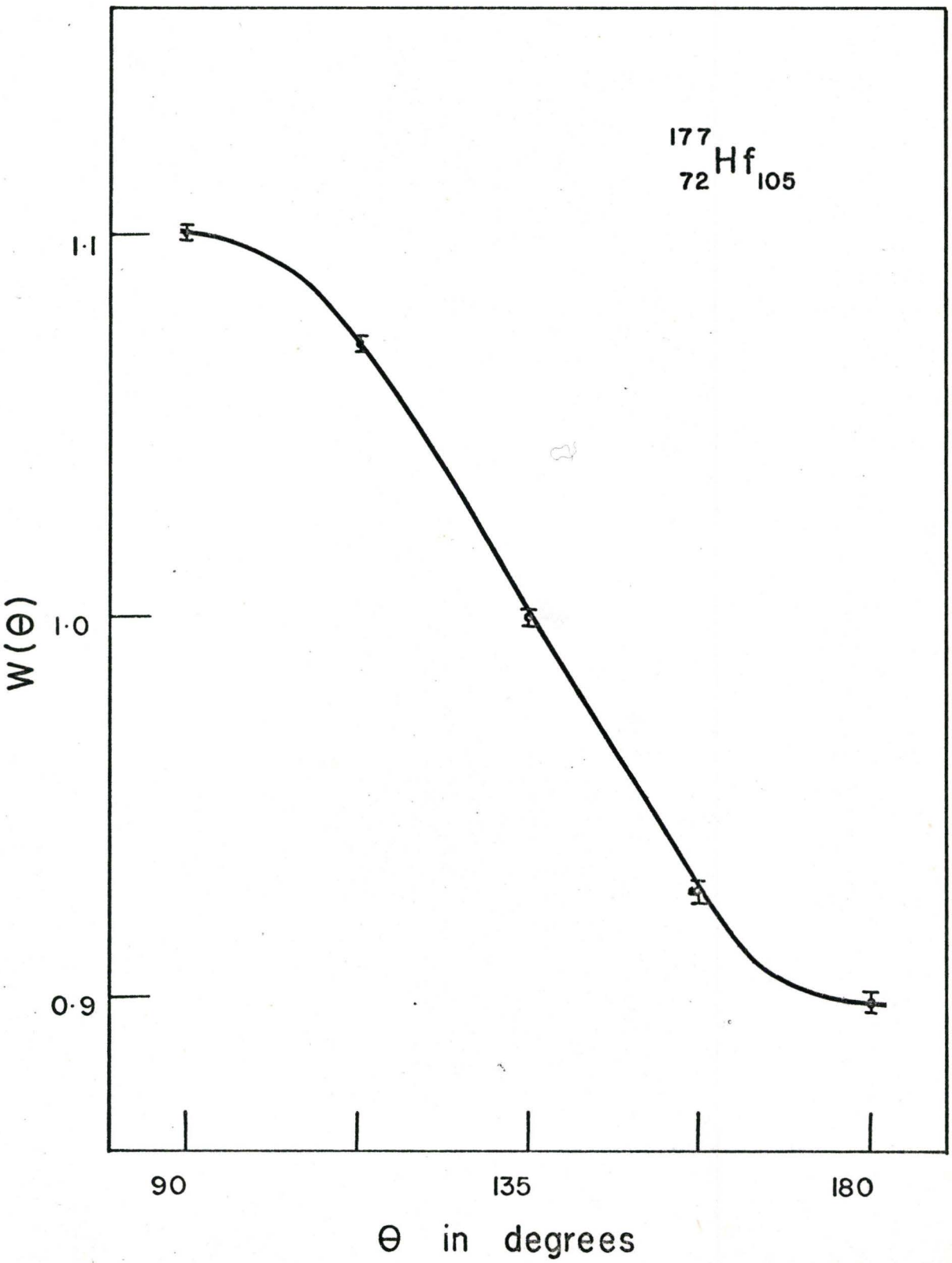
$^{177}_{72}Hf_{105}$
1·1
1·0
0·9
W(Θ)
90
135
180
Θ in degrees

Figure 10

The angular correlation pattern for the

250-71 keV cascade

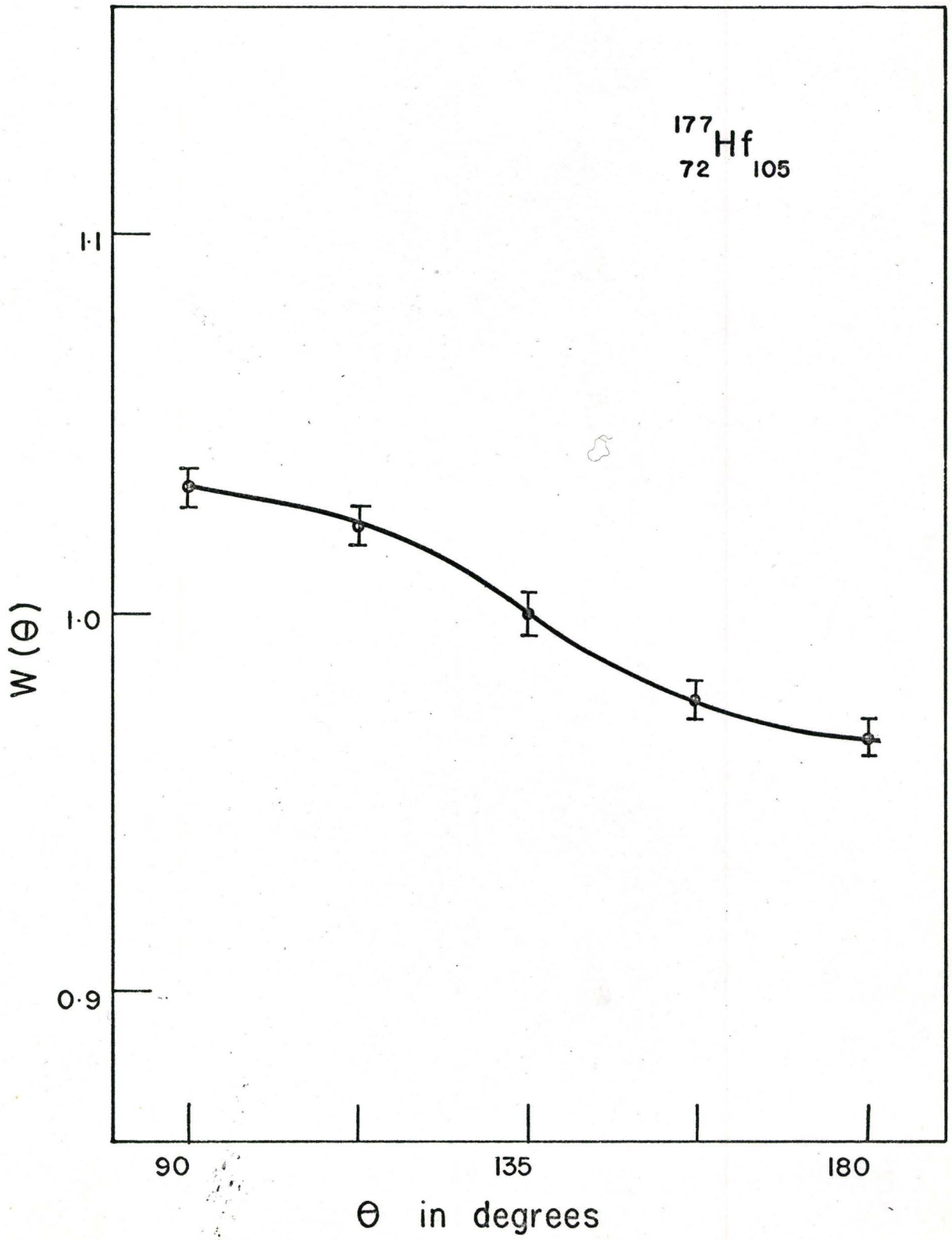
$^{177}_{72}Hf_{105}$
1·1
1·0
0·9
W (Θ)
90
135
180
Θ in degrees

magnetically saturated, the rotation, R, for the first excited state of ^{177}Hf, was measured as a function of magnet current. The result is shown in Figure 12. After these experiments the value of R, for the second excited state, was measured.

6.4 Measurement of g-factors

The values for R/2, for the two cascades studied in this experiment, are shown in Table 1.

Host	Cascade	R/2	ωτ
Gd	208-113	(.033 ± .001)	- (0.187 ± .006)
Gd	71-250	(.0032± .001)	- (0.055 ± .018)

The rotation angles ωτ are obtained using the relation

$$R = (2b_2)(2\omega\tau)/[1 + (2\omega\tau)^2]$$

The magnetic moment of the ground state of ^{177}Hf has been measured by optical methods and has been found to be

$$\mu = (0.61 \pm 0.03) \qquad \text{[Speck,1959]}$$

The g-factor for the first excited state has been measured by angular correlation techniques by Manning [1960] and by Matthias [1962] and was found to be

$$g_{9/2} = (0.235 \pm .006).$$

Figure 11

R as a function of magnet current

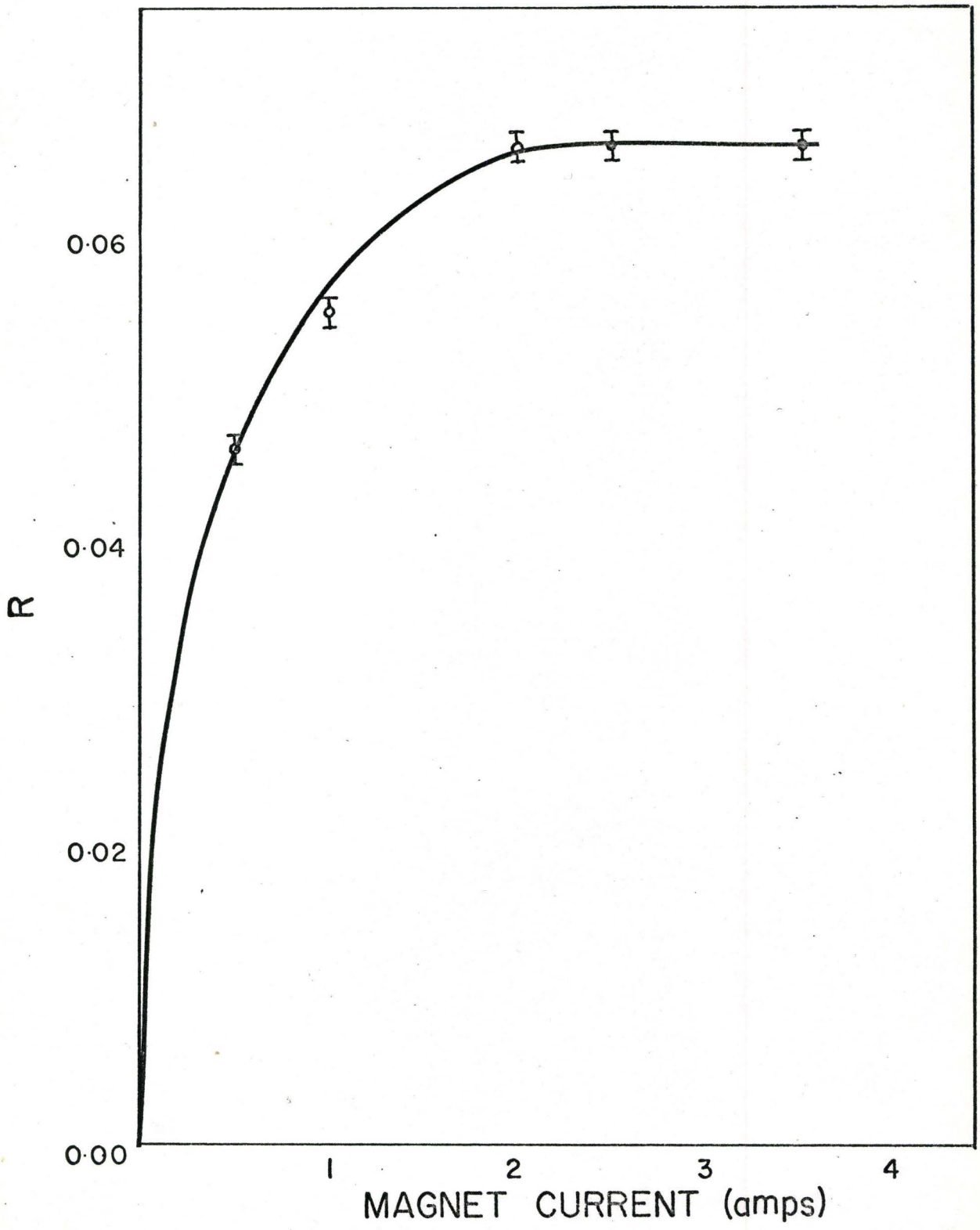
0·06
0·04
0·02
0·00
R
1
2
3
4
MAGNET CURRENT (amps)

The half lives of the first two excited states of ^{177}Hf have been measured:

$$113 \text{ keV level: } T_{1/2} = (0.52 \pm 0.03) \times 10^{-9} \text{ sec}$$

$$250 \text{ keV level: } T_{1/2} = (0.10 \pm 0.02) \times 10^{-9} \text{ sec.}$$

By comparing the measured values of $\omega\tau$ and using the values of the mean lives of the first and the second excited states, one may calculate the g-factor for the second excited state from the relation,

$$\frac{(\omega\tau)^{Gd}_{250}}{(\omega\tau)^{Gd}_{113}} = \frac{g_{11/2}\ \tau_{250}}{g_{9/2}\ \tau_{113}} .$$

Hence,

$$g_{11/2} = (.346 \pm .087).$$

This value of the g-factor does not depend on a calculation of the hyperfine field causing the rotation.

6.5 Hyperfine Fields

The internal field is obtained by comparing the measured values of $\omega\tau$ with that measured in an external field. E. Matthias, E. Karlsson and C. A. Lerjefors [1962] used an external field of (53.1 ± .5)k0e, and obtained

$$(\omega\tau)_{Ext} = (0.0416 \pm .002) \text{ rad.}$$

Using these values and the relation,

$$\frac{H_{eff}}{H_{ext}} = \frac{(\omega\tau)_{eff}}{(\omega\tau)_{ext}}$$

The value of H_{eff} is found to be

$$H_{eff} = - (239 \pm 14) \text{ k0e.}$$

Using the relation given in Chapter III for H_{eff}

$$H_{eff} = H_{int} + H_{\ell}$$

and the value of H_{ℓ}, which was 13 k0e, the value for the internal field on ^{177}Hf in gadolinium is found to be

$$H_{int} = -(252 \pm 14) \text{ k0e.}$$

6.6 Discussion

6.6.1 Hyperfine fields

S. G. Cohen, N. Kaplan and S. Ofer [1964] found the value of internal field and their extrapolated value of the field at 77°K was

$$H_{int} = -(350 \pm 30) \text{ k0e.}$$

The measured value is,

$$H_{int} = - (252 \pm 14) \text{ k0e.}$$

There is a large difference between these two values. This

is probably because of the difference in the sources. Cohen prepared the source by neutron irradiation of 99.9% pure lutecium metal which was then introduced homogenously into 99.9% pure gadolinium, by induction melting the metals in a tantalum crucible. The atomic concentration of luticium, in their source, was between 0.3% to 0.8%.

The ^{177}Hf nucleus was also studied under different environment. The internal field on ^{177}Hf in Fe was measured by Brooker and by Becker, and their values were

$$H_{Fe} = - (133 \pm 7) \text{ kOe}$$

and

$$H_{Fe} = -(300 \pm 60) \text{ kOe} \quad \text{respectively.}$$

Both of them use the implantation technique for making their sources, but have obtained quite different values for H_{Fe}. This shows that the internal field is very sensitive to the sources, which are not reproducible.

6.6.2 g-factors

The measured ratio

$$\frac{(\omega\tau)^{Gd}_{250}}{(\omega\tau)^{Gd}_{113}}$$

is

$$0.29 \pm 0.10.$$

and that of Brooker is

$$\frac{(\omega\tau)^{Fe}_{250}}{(\omega\tau)^{Fe}_{113}} = 0.23 \pm 0.05 \ .$$

The weighted average of these two is

$$(0.25 \pm 0.04)$$

so the measured value is not much different from the weighted average.

The ^{177}Hf lies in the middle of a region of highly distorted nuclei ($150 < A < 190$), and hence it can be properly described by the use of the collective model and the strong coupling scheme discussed in Chapter IV. The magnetic moment of a nucleus in the strong coupling approximation depends upon two parameters: g_R, the g-factor corresponding to the angular momentum of the collective rotation, and g_K, the g-factor appropriate to the angular momentum of the intrinsic particle motion.

Now, using equation

$$\mu = \frac{J}{J+1} (g_R + g_K)$$

for ground state, and

$$\mu(J,K) = g_R \frac{J(J+1)-K^2}{(J+1)} + g_K \frac{K^2}{J+1} \qquad K \neq \frac{1}{2}$$

for the excited states, the two parameters g_R and g_K may be calculated from known g-factors for the ground and first excited states.

The g-factors for the ground and first excited states are

$$g_{7/2} = (0.174 \pm .002)$$

$$g_{9/2} = (0.235 \pm .006)$$

and the measured value of $g_{11/2}$ is

$$g_{11/2} = (.346 \pm .087).$$

Now, using the equation given in Chapter IV,

$$g(J,K) = g_R + (g_K - g_R) \frac{K^2}{J(J+1)} .$$

This gives three relations for the two parameters g_K and g_R. Weighting the ground state and the first and second excited states, a least square fit to the data was performed. The resulting values of g_K and g_R were

$$\left.\begin{aligned} g_K &= 0.112 \\ g_R &= 0.314 \end{aligned}\right\} \text{ from least squares}$$

These two parameters may also be calculated from the known g-factors for the ground and first excited states.

The results obtained are

$$g_K = 0.126 \pm .012$$

$$g_R = 0.343 \pm 0.035.$$

Using the three measured g-factors and the two transition rates, $T(M1)_{9/2\to7/2}$ and $T(M1)_{11/2\to9/2}$ the values for g_K and g_R were calculated. The resulting values are given in Table II.

	Experimental	Theoretical
$g_{7/2}$	(.174±.002)	
$g_{9/2}$	(.235±.006)	
$g_{11/2}$	(.346±.087)	0.273*
$T(M1)_{9/2\to7/2}$	(1.25±0.39) 10^7 sec^{-1}	(1.5±.5)10^7 sec^{-1}
$T(M1)_{11/2\to9/2}$	(29.8±20.8) 10^7 sec^{-1}	(4±2)$\times10^7$ sec^{-1}
g_K (using $g_{9/2}$ and $T(M1)_{9/2\to7/2}$)	(0.248±0.09)	0.44
g_R	(0.222±0.08)	0.41
g_K(using $g_{9/2}$ and $T(M)_{11/2\to9/2}$)	(0.289±.112)	
g_R	(0.181±0.83)	

*Using the known g-factors for the ground and first excited states the value for g_K and g_R were obtained. And using these values the value of μ for the second excited state was calculated which gave the value for $g_{11/2}$ equal to 0.273.

Both these calculations using transition rate give values for g_K which are higher than those obtained from measured values of g-factors. This difference may be due to errors in the mixing ratios δ, total conversion coefficients α_T or in the optically measured ground state moment.

As stated previously ^{177}Hf nucleus lies in the middle of the deformed region ($150<A<190$). The intrinsic states of the nucleus are interpreted in the Nilsson scheme [Nilsson 1955]. For the states corresponding to a given Ω, the vectors $|N\ell\Lambda\Sigma\rangle$ with $\Lambda + \Sigma = \Omega$ are used as basic vectors. Where

Ω = the component of intrinsic angular momentum on the body axis.

N = principal quantum number

ℓ = orbital angular momentum quantum number

Λ = the projection of the orbital angular momentum on the symmetry axis

Σ = the projection of the spin on symmetry axis.

The spin projection Σ is of course either $+\frac{1}{2}$ or $-\frac{1}{2}$.

Mottelson and Nilsson [1959] classified the ground state of ^{177}Hf as

$$\frac{7}{2} - [514]$$

in terms of the basis vectors.

The intrinsic g-factor, g_K, can also be calculated from the Nilsson wave functions.

g_K is given by

$$g_K = \frac{1}{2K}(g_s - g_\ell)\sum_\ell (a^2_{\ell,\Omega-\frac{1}{2}} - a^2_{\ell,\Omega+\frac{1}{2}}) + g_\ell$$

where

g_ℓ = the orbital g-factor for the one extra-core nucleon.

g_s = the spin g-factor for the one extra-core nucleon.

In the case of one neutron, $g_\ell = 0$ and $g_s = -3.826$ nuclear magnetons.

The distortion parameter η was determined by Nilsson and was found to be

$$\eta = 5.5 \text{ [Nilsson 1955]}.$$

Using base vectors $|553+\rangle$, $|533+\rangle$, $|554-\rangle$, the value of g_K is found to be $g_K = 0.44$. This value does not agree with the value calculated from the measured g-factors.

The calculation of g_R from the relation

$$g_R = Z/A$$

gives

$$g_R = 0.41.$$

This is again much larger than the value obtained from the measured g-factors.

The explanation of the discrepancies between the theoretical and experimental data is that the magnetic moments

are quite sensitive to small admixtures of states involving core excitations induced by a δ-function two body residual force [Gauvin 1958]. One of the significant points of this effect is that the magnetic moments always go inward from the Schmidt lines. Blin-Stoyle [1957] interpreted this general trend, as a partial quenching of the nucleon's intrinsic magnetic moment.

For ^{177}Hf, this would suggest that the free neutron moment should be less than the free neutron moment of -3.286 nuclear magnetons. The deviation of the static nuclear moment from single particle estimates may be due to spin-polarization of the even nuclear core by the unpaired extra-core nucleon.

Summary

The experiment was intended to measure the internal field on hafnium in gadolinium and to measure the g-factor of the 250 keV second excited state.

The results were as follows.

$$H_{int} = - (252 \pm 14) \text{ kOe}$$

$$g_{11/2} = (0.346 \pm .087)$$

The measured g-factor is about 23 percent higher than the value predicted using the g-factors of the ground and first excited states.

The technique of making an alloy of two rare earth metals gives satisfactory results. It should be used to allow the studies of all those elements which are soluble in rare earth metals.

APPENDIX

NUCLEAR DATA FOR ^{177}Hf

113 keV Level-:

$\tau_{113} = (0.75 \pm 0.03) \times 10^{-9}$ sec [Bird 1962]

$\delta^2_{9/2 \to 7/2} = (24 \pm 5)$ [N.D.S.]

$\alpha_T = (3.27 \pm 0.3)$ [N.D.S.]

$g_{9/2} = (0.235 \pm .006)$ [Matthias 1962]

250 keV Level:-

$\tau_{250} = (0.14 \pm 0.03) \times 10^{-9}$ sec [N.D.S.]

$\delta^2_{11/2 \to 9/2} = (10 \pm {}^{14}_{5})$ [Boer 1959]

$\alpha_T = (1.18 \pm 0.12)$ [N.D.S.]

BIBLIOGRAPHY

Aeppli, H., Bishop, A.S., Frauenfelder, H., Water, M. and Zunti, W., Phys. Rev. 82, 550 (1951).

Alder, K. and Stech, B. Phys. Rev. 107, 728 (1957).

Bernstein, E.M. and DeBoer, J. Nucl. Phys. 18, 40 (1960).

Birk, M., Blaugrund, A.E., Goldring, G., Skurnik, E.Z., Sokolowski, S.J., Phys. Rev. 126, No. 2, 726 (1962).

Blin-Stoyle, R.J., Theories of Nuclear Moments, Oxford University Press, London, 1957.

Bosch, D., Pobell, F., Phys. Letts. 22, 262 (1967).

Brady, E.L. and Deutsch, M., Phys. Rev. 72, 870 (1947).

Brooker, W.H., Masters Thesis, McMaster University, 1967.

Campbell, I.A., Proc. Phys. Soc. 89, 71 (1966).

Cohen, S.G., Proc. Int. Conf. on Magnetism, 233 (1964).

Chow, Phys. Rev. Letts. 15, 369 (1965).

Cohen, S.G., Phys. Letts. 7, 91 (1963).

Deutch, B.I., Hornshoj, P., Nielson, K. Bonde, Boehm, F., Phys. Letts. 21, No. 6, 659 (1966).

Ferentz and Rosenzweig, appendix 3 in Perturbed Angular Correlations, E. Karlsson, E. Matthias and K. Siegbahn ed., North-Holland Publ. Co., Amsterdam, 1964.

Frauenfelder, H., Steffen, R.M., in Alpha-Beta-and Gamma-Ray Spectroscopy, Volume II, K. Siegbahn ed., North-Holland Publ. Co., Amsterdam, 1966.

Frauenfelder, H. and Scherrer, P., Phys. Acta. 25, 239 (1952).

Goertzel, G., Phys. Rev. 70, 897 (1946).

Gschneidner, K.A., Rare Earth Alloys, D. Van Nostrand Co. Ltd., Princeton, New Jersey, 1961.

Hamilton, D.R., Phys. Rev. 58, 122 (1940).

Hansen, O., Nucl. Phys. 25, 634 (1961).

Hume-Rothery, W., Structure of Metal and Alloys, Institute of Metals, London, 1947.

Manning, G. and Rogers, J.D., Nucl. Phys. 15, 166 (1960).

Marshall, W., Phys. Rev. 110 (G), 1280 (1958).

Matthias, E., Karlsson, E. and Lerjefors, C.A., ARkiv for Fysik, 22, No. 8, 139 (1962).

Mottelson, B.R., and Nilsson, S.G., Mat. Pys. Skr. Dan. Selsk., 1, No. 8 (1959).

Murray, J., Ph.D. Thesis, McMaster University, 1967.

Nilsson, S.G., Dan Mat. Fys. Medd., 29, 16 (1955).

Nuclear Data Sheets, 1963, Nat'l. Acad. Sci.-Nat'l Res. Council, Washington, N.R.C.

Preston, M.A., Physics of the Nucleus, Addison-Wesley Publishing Co., Reading, Mass., 1962.

Watson, R.E. and Freeman, J.A., Phys. Rev. 123(b), 2027 (1961).

Yang, C.N., Phys. Rev. 74, 764 (1948).

Yates, M.J.L., appendix 4 in Perturbed Angular Correlations, E. Karlsson,E. Matthias and S. Siegbahn, ed., North-Holland Publ. Co., Amsterdam, 1964.